

Interparticle interactions in composites of nanoparticles of ferrimagnetic (γ -Fe₂O₃) and antiferromagnetic (CoO, NiO) materials

C. Frandsen,¹ C. W. Ostefeld,¹ M. Xu,^{1,*} C. S. Jacobsen,¹ L. Keller,² K. Lefmann,³ and S. Mørup¹

¹*Department of Physics, Technical University of Denmark, DK-2800 Kgs. Lyngby, Denmark*

²*Laboratory for Neutron Scattering, ETHZ & PSI, CH-5232 Villigen PSI, Switzerland*

³*Materials Research Department, Risø National Laboratory, DK-4000 Roskilde, Denmark*

(Received 8 March 2004; revised manuscript received 1 July 2004; published 26 October 2004)

The magnetic properties of mixtures of ferrimagnetic γ -Fe₂O₃ (maghemite) and antiferromagnetic NiO or CoO nanoparticles have been studied by use of ⁵⁷Fe Mössbauer spectroscopy, neutron powder diffraction and magnetization measurements. The studies showed that the interaction with antiferromagnetic particles has a significant influence on the magnetic properties of the γ -Fe₂O₃ nanoparticles. It was found that mixing the γ -Fe₂O₃ nanoparticles with NiO nanoparticles resulted in a faster superparamagnetic relaxation and a reduced coercivity compared to a sample consisting solely of γ -Fe₂O₃ nanoparticles. On the contrary, mixing of γ -Fe₂O₃ nanoparticles with CoO nanoparticles resulted in a suppression of the relaxation and an increase in coercivity. These results suggest that the properties of the ferrimagnetic γ -Fe₂O₃ nanoparticles are influenced by the anisotropy of their neighboring antiferromagnetic particles. The dominating type of magnetic interaction between the particles in the composites seems to be exchange interaction between surface atoms of neighboring particles.

DOI: 10.1103/PhysRevB.70.134416

PACS number(s): 75.50.Tt, 75.75.+a, 76.80.+y, 75.60.Ej

I. INTRODUCTION

Interparticle interactions between magnetic nanoparticles can have strong influence on the magnetic properties; in particular, the superparamagnetic relaxation of the particles can be significantly affected by interactions.^{1–18} The influence of dipolar interactions between ferromagnetic or ferrimagnetic nanoparticles has been studied in, for example, frozen ferrofluids with different interparticle distances. Weak dipole interactions can lead to faster relaxation,¹² whereas strong interactions may result in slowing down of the relaxation and eventually to a divergence of the superparamagnetic relaxation time at a critical temperature, which increases with increasing strength of the interaction.^{1,2,13–16} Below this critical temperature the samples have many similarities with spin-glasses.^{2–5}

Dipolar interactions between antiferromagnetic nanoparticles are typically too weak to have any significant influence on the relaxation behaviour, even if the particles are in close contact.^{6,7} Still, Mössbauer spectroscopy studies have shown that antiferromagnetic nanoparticles in close proximity often have their superparamagnetic relaxation suppressed compared to noninteracting particles.^{7,9–11} This suggests that exchange interactions between surface atoms of neighboring particles can be significant.

Exchange interaction across interfaces between ferro- or ferrimagnetic materials and antiferromagnetic materials has great technological importance because it can lead to enhanced coercivity and shifted hysteresis loops, known as “exchange bias,” due to the pinning of the magnetization of the ferromagnet by the antiferromagnet.^{19,20} Studies of thin films of Fe₃O₄ interlayered with either CoO or NiO have revealed another interesting phenomenon, namely that the interactions between the two materials can result in a substantial increase of the Néel temperature of CoO and

NiO.^{21,22} Most of the studies of exchange interaction across interfaces have been focused on thin film structures, because of their use in spin valves, which play an important role in, for example, read heads in present day computers. It has recently been shown that the exchange coupling of ferromagnetic nanoparticles to an antiferromagnetic environment can lead to a greatly enhanced anisotropy and this may be utilized to increase the information density in magnetic recording media.²³ Studies of annealed self-assembled nanoparticles have revealed strong exchange coupling, which can be used for creating permanent magnets.²⁴ In other studies, nanoparticles of ferro- or ferrimagnetic materials have been mixed with antiferromagnetic nanoparticles by ball-milling.^{25–27} When using this preparation technique, nanoparticles of the different materials may be welded together and therefore come in close contact such that exchange coupling between the particles can be significant. In these studies, it was found that interaction with the antiferromagnetic particles can result in both an enhanced coercivity and a nonzero exchange bias.

We have earlier investigated the influence of interparticle interactions between antiferromagnetic nanoparticles of different materials, prepared by drying aqueous suspensions of the particles.^{9,10} With this preparation technique one might expect the interparticle interactions to be weak. However, Mössbauer studies of pure α -Fe₂O₃ (Refs. 7 and 10) or ⁵⁷Fe-doped NiO (Ref. 11) nanoparticles have shown that the superparamagnetic relaxation is significantly suppressed in samples prepared by drying aqueous suspensions. The studies of samples of nanoparticles of different materials also gave some unexpected results.^{9,10} For example, mixing of α -Fe₂O₃ nanoparticles with CoO nanoparticles resulted in a strong suppression of the superparamagnetic relaxation, whereas mixing α -Fe₂O₃ nanoparticles with NiO nanoparticles had the opposite effect. Furthermore, surprisingly it

was found that mixing with NiO particles resulted in a Morin transition in 9 nm α -Fe₂O₃ nanoparticles, although this magnetic phase transition normally is absent in α -Fe₂O₃ particles with diameters below ~ 20 nm. In this paper, we present the results of studies of mixtures of 7 nm ferrimagnetic γ -Fe₂O₃ nanoparticles with antiferromagnetic NiO or CoO nanoparticles. By use of Mössbauer spectroscopy, we have studied the influence of interactions on the relaxation of the γ -Fe₂O₃ nanoparticles. The results are qualitatively similar to those obtained in our previous studies of mixtures with α -Fe₂O₃ nanoparticles.^{9,10} Magnetization measurements on the composites show that interparticle interactions affect also the coercivity of the γ -Fe₂O₃ nanoparticles. This result supports that there is a strong exchange interaction between the particles in the samples.

II. MÖSSBAUER SPECTRA OF NONINTERACTING AND INTERACTING MAGNETIC NANOPARTICLES

The magnetic anisotropy of an isolated magnetic nanoparticle is often assumed uniaxial with a magnetic anisotropy energy density given by

$$E = K \sin^2 \theta, \quad (1)$$

where K is the magnetic anisotropy energy constant, and θ is the angle between the (sublattice) magnetization direction and an easy direction of magnetization. Very small particles may perform superparamagnetic relaxation [i.e., thermal fluctuations of the (sublattice) magnetization between the two minima at $\theta=0^\circ$ and $\theta=180^\circ$] with a relaxation time, τ , given by the Néel-Brown expression^{28,29}

$$\tau = \tau_0 \exp(KV/k_B T), \quad (2)$$

where V is the particle volume, k_B is Boltzmann's constant, and T is the temperature. τ_0 is typically in the range 10^{-11} – 10^{-9} s. In nanoparticles, for which τ_0 is small ($\sim 10^{-11}$ s) compared to the time scale of Mössbauer spectroscopy, $\tau_M \sim 5 \cdot 10^{-9}$ s, a typical (i.e., not truly monodisperse) particle size distribution will result in a very wide range of relaxation times at temperatures where the average relaxation time is close to τ_M . This is due to the exponential dependence of τ on V . Therefore, close to the blocking temperature, only a tiny fraction of the particles will have relaxation times close to τ_M , which would give rise to broad components in the spectra.^{10,30} Instead, the spectra will mainly consist of a superposition of a sextet with narrow lines, representing those particles, which are below their blocking temperature ($\tau \gg \tau_M$), and a sharp central doublet or singlet, representing those particles which exhibit fast superparamagnetic relaxation ($\tau \ll \tau_M$). However, if τ_0 is of the order of 10^{-10} – 10^{-9} s, a large fraction of the particles in a sample has relaxation times comparable to the time scale of Mössbauer spectroscopy in a temperature range where $KV/k_B T$ is small. This will result in spectra with broadened lines around the blocking temperature.

If the particles are in close proximity, Eq. (1) may be replaced by^{7,8,10}

$$E = K \sin^2 \theta - \mathbf{M} \cdot \mathbf{B}_{\text{int}}, \quad (3)$$

where \mathbf{B}_{int} is an effective interaction field, which may have its main contributions from exchange interactions with neighboring magnetic particles, and \mathbf{M} is the (sublattice) magnetization. If the second term in Eq. (3) is predominant, there will be only one energy minimum of the magnetic energy, and the magnetization vector may then fluctuate around the direction of the effective interaction field. In this case the average of the magnetic hyperfine field has a finite value, and the Mössbauer spectra will therefore be magnetically split. However, even for very fast fluctuations, the spectra will have broad lines because of the distribution of effective interaction fields in samples of interacting nanoparticles.^{7,8,10} Only at high temperatures, where the thermal energy becomes comparable to or larger than the interparticle interaction energy, there will be a doublet or singlet component in the spectra.

III. EXPERIMENTAL DETAILS

γ -Fe₂O₃ nanoparticles were prepared by oxidation at ambient conditions of Fe₃O₄ nanoparticles, which were made by co-precipitation of Fe(II) and Fe(III) from an aqueous solution of 2.0 M Fe(NO₃)₃ and 1.0 M FeSO₄ by adding a 1.0 M aqueous solution of NaOH. The particles were washed through several steps with H₂O and acetone. After washing, the particles in a part of the sample were coated with oleic acid and suspended in heptane in order to minimize interparticle interactions. The particles in the remaining part of the sample were left uncoated and freeze-dried.

NiO nanoparticles were prepared by thermal decomposition of Ni(OH)₂ at 325 °C in air for 3 h, similar to the preparation described in Ref. 11.

CoO nanoparticles were prepared by two different methods. A sample, called CoO-ann, was prepared by heating cobalt acetate in an argon atmosphere at 300 °C for 4 h. This sample contained a minor impurity of metallic Co. Another sample of CoO particles, CoO-bm, was prepared by high-energy ball-milling of a 1:1 molar ratio mixture of Co₃O₄ and Co in argon for 115 h. This preparation method seems to be a convenient way to produce pure and fairly small CoO particles.

Mixtures of nanoparticles of γ -Fe₂O₃ with NiO or CoO (1:1 by weight, unless otherwise indicated) were prepared by suspending the particles in distilled water, and subsequently exposing them to intense ultrasound with the aim to break apart agglomerates and to obtain a homogeneous mixture. The mixed samples were left to dry in open petri dishes in air at room temperature for about 2 days or at 200 °C for 2 h. The dried powders were collected from the petri dishes with a plastic spatula and packed into sample containers. For Mössbauer spectroscopy and magnetization measurements, the powders were tightly packed. In particular for magnetization measurements, where magnetic fields of up to 1 T were applied, the powders were densely compacted to a coherent solid, with the aim to avoid rotation of the particles during measurements. No binding materials such as epoxy were added to the powders in order not to affect the interparticle interactions.

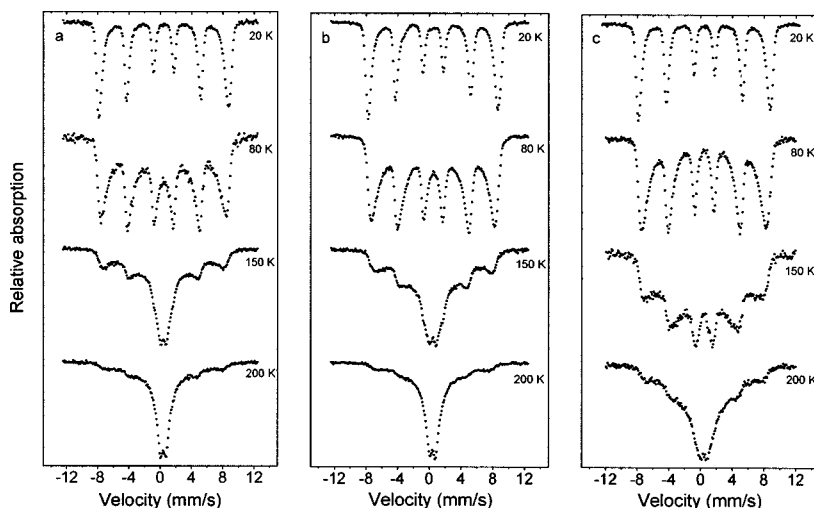


FIG. 1. ^{57}Fe -Mössbauer spectra obtained at the indicated temperatures of samples of pure 7 nm $\gamma\text{-Fe}_2\text{O}_3$ particles. (a) Coated with oleic acid and suspended in heptane (b) uncoated, freeze-dried, (c) uncoated, dried at room temperature.

X-ray diffraction (XRD) was performed using a PW 1390 Philips diffractometer with a $\text{Cu } K_\alpha$ radiation source.

Transmission electron microscopy (TEM) images were obtained by a Philips EM 430 operated at voltages up to 300 kV.

Mössbauer spectra were obtained using conventional constant acceleration spectrometers with sources of ^{57}Co in rhodium. The instruments were calibrated by use of a $12.5 \mu\text{m}$ foil of $\alpha\text{-Fe}$. Velocities and isomer shifts are given relative to the centroid of the calibration spectrum.

Neutron powder diffraction measurements were performed on the DMC diffractometer at the Swiss Spallation Neutron Source, Paul Scherrer Institute, Villigen, Switzerland. The diffractometer uses a multi-detector, which spans a two-theta angle of 80° with a detector separation of 0.2° . We used a wavelength of 4.2 \AA for the measurements. By using a two-theta starting angle of 33° , we were able to record, for CoO, the antiferromagnetic ($1/2, 1/2, 1/2$) reflection at 1.28 \AA^{-1} , the magnetic ($1/2, 1/2, 3/2$) reflection at 2.45 \AA^{-1} , and the structural (111) reflection at 2.56 \AA^{-1} .

Magnetic hysteresis loops were measured by use of a vibrating sample magnetometer with a superconducting coil magnet. The samples were enclosed in copper cylinders with typical sample masses of 125 mg. The instrument was calibrated using the known magnetic saturation moment of a cobalt sample. Measurements were performed at temperatures between 5 K and 310 K in applied fields up to 1 T. Field cooled hysteresis curves were obtained by cooling in a field of 1 T over less than 30 min and then recording the loop starting from 1 T.

IV. RESULTS

A. X-ray and neutron powder diffraction

The average particle diameter was estimated for all samples from the XRD data by use of the Scherrer formula. In the analysis we neglected the possible influence of strain on the line broadening. This may result in an underestimate of the particle size, especially for the ball-milled sample. The analysis showed that the $\gamma\text{-Fe}_2\text{O}_3$ particles had an average diameter of about 7 nm. The particles of the CoO-ann

sample had an average diameter of 16 nm, whereas the particles of the CoO-bm sample had a diameter of about 10 nm. The mean diameter of the NiO particles was found to be about 5 nm. The results of the XRD analysis were confirmed by electron microscopy studies. TEM studies further showed that the $\gamma\text{-Fe}_2\text{O}_3$ and CoO particles are pseudo-spherical in shape, while the NiO particles were plate-shaped with a diameter of about 17 nm and a thickness of about 3 nm.

Neutron powder diffraction data of the two CoO samples, CoO-ann and CoO-bm showed that the Néel temperatures of the nanoparticles are very close to the bulk value (293 K). This was found from following the decrease in integrated intensity of the antiferromagnetic ($1/2, 1/2, 1/2$) reflection. Previous neutron powder diffraction studies of NiO nanoparticles,³¹ which are similar to the NiO particles studied here, have shown that the Néel temperature of these plate-shaped nanoparticles is about 60 K lower than the bulk value (523 K).

By use of neutron diffraction, we have not been able to resolve a possible increase in the Néel temperature of the CoO nanoparticles above the bulk value, when in composites with iron oxides with higher ordering temperatures, such as reported for CoO/ Fe_3O_4 multilayer structures.²² For both $\gamma\text{-Fe}_2\text{O}_3 + \text{CoO}$ and $\gamma\text{-Fe}_2\text{O}_3 + \text{NiO}$ composites, overlapping reflection lines made it impossible to determine the critical temperatures of CoO or NiO. Complementary, we have looked at samples of $\alpha\text{-Fe}_2\text{O}_3 + \text{CoO}$, composites in which significant interparticle interactions have previously been observed by Mössbauer spectroscopy.^{9,10} In such composites, the diffraction lines of the two components can clearly be resolved and it was seen that the antiferromagnetic reflection of CoO vanished at a temperature close to 300 K. Thus the Néel temperature of CoO nanoparticles does not seem to increase due to the interparticle interactions.

B. Mössbauer spectroscopy

Figure 1 shows Mössbauer spectra of samples consisting solely of 7 nm $\gamma\text{-Fe}_2\text{O}_3$ nanoparticles. The spectra shown in Fig. 1(a) were obtained from a sample of particles coated with oleic acid. These spectra show an evolution with tem-

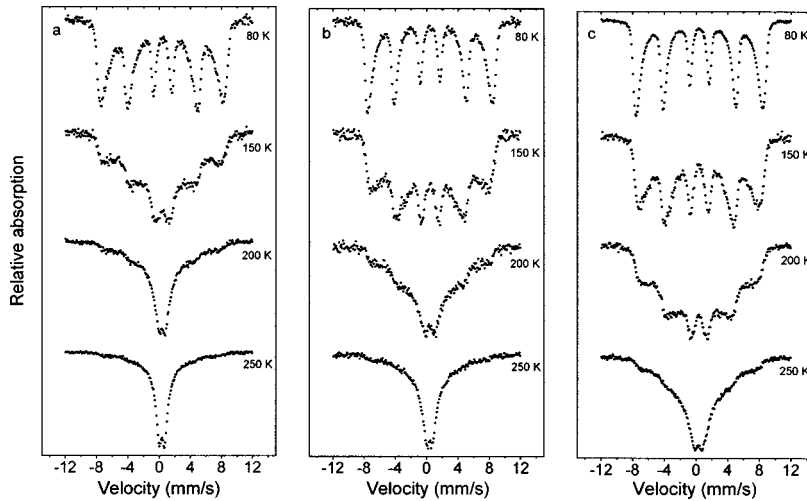


FIG. 2. ^{57}Fe -Mössbauer spectra obtained at the indicated temperatures of 7 nm $\gamma\text{-Fe}_2\text{O}_3$ particles (a) mixed with NiO nanoparticles and dried at room temperature, (b) mixed with NiO nanoparticles and dried at 200°C, and (c) pure $\gamma\text{-Fe}_2\text{O}_3$ particles dried at 200°C.

perature, which is typical for noninteracting or weakly interacting superparamagnetic particles, i.e., a coexistence of a doublet and a sextet, with the relative area of the doublet increasing with increasing temperature at the expense of the sextet. In the spectra, where both a doublet and a sextet are present (e.g., at 150 K), neither of them have narrow lines. In spectra of noninteracting nanoparticles of $\alpha\text{-Fe}_2\text{O}_3$ the lines of both the sextet and the doublet are considerably narrower.^{32,33} The difference between the two iron oxides can be explained by the different values of the parameter τ_0 in the two materials as discussed in Sec. II. A small value of τ_0 results in a very wide distribution of relaxation times in the temperature range where the Mössbauer spectrum gradually transforms from a sextet to a doublet such that most of the particles have relaxation times that are either much longer or much shorter than τ_M . This is the case for $\alpha\text{-Fe}_2\text{O}_3$ nanoparticles where $\tau_0 \sim 10^{-11}$ s.³²⁻³⁴ In 7 nm $\gamma\text{-Fe}_2\text{O}_3$ particles the value of τ_0 is of the order of $5 \cdot 10^{-10}$ s.³⁵ This means that for small values of the parameter $KV/k_B T$ the particles will have relaxation times of the order of 10^{-9} – 10^{-8} s. This results in broad lines in the Mössbauer spectra.^{10,30}

The spectra in Fig. 1(b) were obtained from a sample of uncoated particles, which were freeze-dried. These spectra are quite similar to those shown in Fig. 1(a), indicating that the interparticle interactions only play a minor role in this sample.

Figure 1(c) shows spectra of a sample of uncoated particles, which was prepared by suspending the freeze-dried particles in water by exposing them to ultrasound and then allowing them to dry at room temperature. In these spectra the superparamagnetic relaxation is to a large extent suppressed at intermediate temperatures. For example, at 150 K only a sextet with broad lines is visible in contrast to Figs. 1(a) and 1(b) in which an intense doublet is also visible at this temperature. Such a suppression of the superparamagnetic relaxation is a typical feature of nanoparticles with a significant interparticle magnetic interaction.^{7-11,17} A comparison of the spectra in Figs. 1(b) and 1(c) shows that the way in which the samples are prepared plays a crucial role for the magnetic properties of nanopowders.

Mössbauer spectra of a sample consisting of a mixture of $\gamma\text{-Fe}_2\text{O}_3$ and NiO nanoparticles, prepared by exposing an

aqueous suspension of the particles to ultrasound followed by drying at room temperature, are shown in Fig. 2(a). Compared to the spectra of the pure $\gamma\text{-Fe}_2\text{O}_3$ particles, prepared in the same way [Fig. 1(c)], the spectra of the mixture indicate a faster relaxation of the $\gamma\text{-Fe}_2\text{O}_3$ particles. This is in particular evident when comparing the spectra obtained at 150 and 200 K of the two samples. Spectra of mixtures of $\gamma\text{-Fe}_2\text{O}_3$ and NiO nanoparticles, dried at 200°C [Fig. 2(b)], show less influence of relaxation, presumably because of a stronger interparticle interaction induced by the heating. For comparison, Fig. 2(c) shows spectra of the pure $\gamma\text{-Fe}_2\text{O}_3$ nanoparticles, dried at the same temperature. These spectra also suggest an enhanced interaction compared to the sample dried at room temperature, but the spectra of samples containing NiO are much more influenced by relaxation than the samples of pure $\gamma\text{-Fe}_2\text{O}_3$ nanoparticles.

Figure 3 shows spectra of a mixture of $\gamma\text{-Fe}_2\text{O}_3$ and CoO (CoO-ann) nanoparticles, prepared by exposing an aqueous

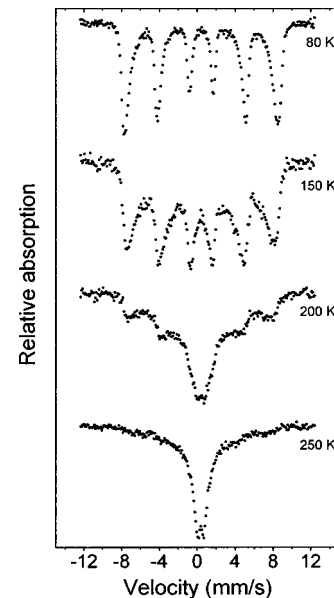


FIG. 3. ^{57}Fe -Mössbauer spectra obtained at the indicated temperatures of 7 nm $\gamma\text{-Fe}_2\text{O}_3$ particles mixed with CoO-ann nanoparticles at room temperature.

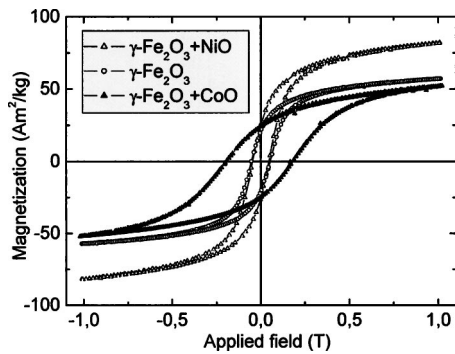


FIG. 4. Hysteresis loops of $\gamma\text{-Fe}_2\text{O}_3$, $\gamma\text{-Fe}_2\text{O}_3+\text{CoO-bm}$ and $\gamma\text{-Fe}_2\text{O}_3+\text{NiO}$ at 5 K. The magnetization is given per mass unit of $\gamma\text{-Fe}_2\text{O}_3$ in the samples.

suspension to ultrasound with subsequent drying at room temperature. A comparison with the spectra in Figs. 1(c) and 2(a) shows that CoO has the opposite effect of NiO, i.e., it leads to suppression of the superparamagnetic relaxation in the $\gamma\text{-Fe}_2\text{O}_3$ particles. This is most clearly seen in the spectra obtained at 150 K.

In order to study the influence of the method for preparation of CoO and the mixing ratio in samples with $\gamma\text{-Fe}_2\text{O}_3$ and CoO nanoparticles, we prepared samples with different ratios of the two oxides. In this series we used the CoO that was prepared by ball milling (CoO-bm) and we prepared samples with 75%, 50%, 25%, and 10% $\gamma\text{-Fe}_2\text{O}_3$. The spectra of all these samples did not differ much and they were very similar to those in Fig. 3. Thus, a relatively small amount of CoO nanoparticles is sufficient to produce the interaction effect. Moreover, the different preparation techniques and the different average particle size of the two CoO samples have little influence on the interaction effects.

Drying mixtures of $\gamma\text{-Fe}_2\text{O}_3$ and CoO nanoparticles with different mixing ratios at 200°C did not result in systematic variations of the relaxation behavior, but XRD studies of the samples showed that part of the CoO had oxidized to Co_3O_4 , which is paramagnetic at temperatures above 80 K. Therefore, the samples containing CoO dried at room temperature and at 200°C cannot be compared directly.

C. Magnetization measurements

Figure 4 shows hysteresis loops of the pure $\gamma\text{-Fe}_2\text{O}_3$ nanoparticles and of the composites of $\gamma\text{-Fe}_2\text{O}_3+\text{NiO}$ and $\gamma\text{-Fe}_2\text{O}_3+\text{CoO-bm}$ nanoparticles at 5 K after cooling in zero-field. All three samples are those prepared by ultrasound treatment of aqueous suspensions followed by drying. The magnetization at 1 T of the sample of pure $\gamma\text{-Fe}_2\text{O}_3$ nanoparticles is about 57 A m²/kg. For each sample, the magnetization is shown per unit mass $\gamma\text{-Fe}_2\text{O}_3$. It can be seen that the NiO particles have a nonzero moment (of about 25 A m²/kg, presumably due to uncompensated spins of the plate-shaped NiO particles), whereas a magnetic moment from CoO particles could not be resolved at the maximum applied field of 1 T. Rather, the magnetization of the $\gamma\text{-Fe}_2\text{O}_3+\text{CoO-bm}$ composite is less than that of the pure $\gamma\text{-Fe}_2\text{O}_3$ nanoparticles. An explanation for the latter could be

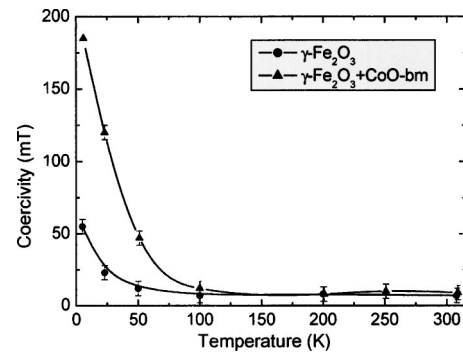


FIG. 5. The coercivity of pure $\gamma\text{-Fe}_2\text{O}_3$ and $\gamma\text{-Fe}_2\text{O}_3+\text{CoO-bm}$ nanoparticles plotted as a function of temperature. The solid lines are guides to the eye.

that the sample of $\gamma\text{-Fe}_2\text{O}_3$ nanoparticles interacting with CoO is not as close to saturation at 1 T as the pure sample of $\gamma\text{-Fe}_2\text{O}_3$. This is supported by the different slopes of the magnetization curves of $\gamma\text{-Fe}_2\text{O}_3$ and $\gamma\text{-Fe}_2\text{O}_3+\text{CoO-bm}$ when approaching 1 T. All three loops are smooth and thus show no sign of having more than one type of contribution, i.e., the composites seem to behave magnetically as single-phase materials indicating that there is a strong exchange interaction between the particles.²⁴ From the loops, we find that the 7 nm $\gamma\text{-Fe}_2\text{O}_3$ particles have a coercivity, $\mu_0 H_C = 55(\pm 2)$ mT, while the composite of $\gamma\text{-Fe}_2\text{O}_3+\text{NiO}$ has a slightly lower value, about $43(\pm 3)$ mT. Quite contrary, for the $\gamma\text{-Fe}_2\text{O}_3+\text{CoO-bm}$ composite, we find that $\mu_0 H_C = 185(\pm 10)$ mT, which is more than three times as large as it is for the sample consisting purely of $\gamma\text{-Fe}_2\text{O}_3$ nanoparticles from the same batch. Thus, the influence of the interparticle interactions on the coercivity can be quite significant.

In Fig. 5, it is shown how the coercivity of the samples of $\gamma\text{-Fe}_2\text{O}_3$ and $\gamma\text{-Fe}_2\text{O}_3+\text{CoO-bm}$ changes with temperature. The difference between the two samples observed at low temperatures diminishes with increasing temperature and at $T \geq 100$ K, the coercivity is similar and almost negligible for the two samples. The fact that the coercivity does not become zero seems to be an effect of the magnetometer.

In order to see if the interaction with the antiferromagnetic particles could be observed directly as a shifted hysteresis loop, i.e., as exchange bias, of the ferrimagnetic $\gamma\text{-Fe}_2\text{O}_3$ nanoparticles, we recorded the loops of the pure $\gamma\text{-Fe}_2\text{O}_3$ and the composites of $\gamma\text{-Fe}_2\text{O}_3+\text{NiO}$ and $\gamma\text{-Fe}_2\text{O}_3+\text{CoO-bm}$ at 5 K after cooling in a field of 1 T from 310 K (i.e., from a temperature above the Néel temperature of CoO and above the blocking temperature of the NiO nanoparticles as determined by Mössbauer spectroscopy studies of similar ⁵⁷Fe-doped NiO nanoparticles^{10,11}). For both the pure $\gamma\text{-Fe}_2\text{O}_3$ sample and the composites we observed small loop shifts, which (in relative values) were nearly identical for the three samples. Therefore, it seems that the loop shifts are not related to exchange coupling at the interface between ferrimagnetic and antiferromagnetic particles, but it is rather an intrinsic property of the $\gamma\text{-Fe}_2\text{O}_3$ nanoparticles. Such a behavior of pure $\gamma\text{-Fe}_2\text{O}_3$ nanoparticles has been reported by Martínez *et al.*³⁶

V. DISCUSSION

Our studies of differently prepared samples of γ -Fe₂O₃ nanoparticles show that the preparation conditions have a great influence on the magnetic properties. Mössbauer studies of an uncoated freeze-dried sample of γ -Fe₂O₃ nanoparticles and an uncoated sample dried at room temperature showed significantly different relaxation behavior. Mixing γ -Fe₂O₃ nanoparticles with NiO nanoparticles results in faster relaxation of γ -Fe₂O₃ particles. However, mixing γ -Fe₂O₃ nanoparticles with CoO nanoparticles had the opposite effect.

It could be argued that the change of relaxation behavior in the composites might be due to a change in the magnetic anisotropy of the maghemite nanoparticles induced by chemisorbed Co²⁺ or Ni²⁺ ions. During the ultrasonic treatment in water, such ions may be dissolved from the CoO or NiO particles. In fact, because Co²⁺ ions have large single-ion anisotropy, chemisorbed Co²⁺ ions might result in an enhanced anisotropy, which could explain the suppression of the relaxation. However, we have prepared samples by drying γ -Fe₂O₃ particles from aqueous solutions of Co²⁺, and we have found no effect on the relaxation. Moreover, in agreement with this, previous studies of α -Fe₂O₃ nanoparticles with chemisorbed Ni²⁺ or Co²⁺ ions have also shown that these ions cannot account for the measured effects in nanocomposites.¹⁰

Dipolar interactions in the nanopowders might play a role for the magnetic properties of the samples, especially since both the γ -Fe₂O₃ and NiO nanoparticles have been found to have significant magnetic moments. The energy of the dipole interaction between two adjacent spherical γ -Fe₂O₃ particles, which are 7 nm in diameter and have a magnetization of 57 A m²/kg, is about 100 K, and for two spherical 5 nm NiO particles with a magnetization of 25 A m²/kg, the dipole interaction energy is about 10 K. These interaction energies might account for some of the observed effects. For instance, the increased relaxation of γ -Fe₂O₃ nanoparticles in the composite of γ -Fe₂O₃+NiO, compared to the pure γ -Fe₂O₃ nanoparticles, could be explained by the reduced interaction energy, when interaction with NiO instead of γ -Fe₂O₃ particles. On the other hand, we have seen how CoO nanoparticles, which have insignificant external magnetic moments, had the most profound influence on the properties of γ -Fe₂O₃ nanoparticles. Therefore, exchange interactions between the particles must be prevalent in the samples. This is also in accordance with the results obtained on anti-ferromagnetic composites.¹⁰

It is remarkable that exchange interactions across the interfaces of nanoparticles in close proximity in a powder are strong enough to result in a significant change in the relaxation and coercivity. If the particles were separated by layers of, for example, adsorbed water or if there are mismatches between the directions of sublattice magnetizations, one would expect the interparticle exchange interaction to be small (in insulators, one would not expect exchange coupling if the magnetic materials are separated by a nonmagnetic spacer, but this can be the case in metallic systems³⁷). Further, if a particle interacts with several neighbors, one might also expect that the interaction fields would partly compen-

sate. However, since the drying method influences the strength of interparticle interaction [Figs. 1(b) and 1(c)], the results suggest that during drying of aqueous suspensions the particles are brought in close proximity in such a way that the magnetic interaction strength is large. Here, van der Waals or magnetic forces may play a role.

It is interesting that mixing γ -Fe₂O₃ particles with NiO and CoO nanoparticles have the opposite effects on the relaxation of γ -Fe₂O₃ particles. Similar results were found for mixtures of α -Fe₂O₃ nanoparticles with NiO and CoO nanoparticles.^{9,10} We believe that the observed different influences of NiO and CoO nanoparticles are mainly a consequence of their different anisotropy energies. The NiO particles have very small volumes and the magnetic anisotropy constant of NiO is not very large. Therefore, the NiO particles are expected to have small magnetic anisotropy energy. It is possible that the effective anisotropy of the NiO particles is too small compared to that of the γ -Fe₂O₃ particles to induce exchange coupling effects.³⁸ Mössbauer studies of a similarly prepared sample of NiO, which was doped with ⁵⁷Fe, showed that the NiO particles are superparamagnetic with a blocking temperature of about 120 K.¹¹ When the γ -Fe₂O₃ particles are separated by NiO particles, their magnetic coupling to other γ -Fe₂O₃ particles may therefore be weakened. The CoO particles are larger than the NiO particles and they have larger magnetic anisotropy energy constant. Therefore, a γ -Fe₂O₃ particle, which is coupled to a CoO particle, cannot relax in the same way as it could when it was isolated or only in contact with other γ -Fe₂O₃ particles. It may, to a certain extent, have to follow the fluctuations of the magnetization direction of the CoO particles, which have slow relaxation because of the large anisotropy energy. The different morphologies of the NiO and CoO particles also may lead to differences in the physical contact with the γ -Fe₂O₃ particles, and this can also play a role for the exact strength of interparticle coupling.

The magnetization measurements indicate, in agreement with Mössbauer spectroscopy studies, that exchange anisotropy influences the properties of the γ -Fe₂O₃ nanoparticles. The coercivity of the γ -Fe₂O₃ nanoparticles was tripled at low temperatures when interacting with CoO nanoparticles, while it was slightly reduced when interacting with NiO nanoparticles. This can be explained by the different anisotropies of the CoO and NiO particles, which the γ -Fe₂O₃ particles apparently couple to. At increasing temperatures we have seen how the coercivity of γ -Fe₂O₃+CoO decreases. This is presumably because the coupled CoO and γ -Fe₂O₃ particles perform superparamagnetic relaxation. The temperature range where it happens in the magnetization measurements is somewhat lower than the temperature range, where the Mössbauer spectra change from a sextet to a doublet, as expected due to the different time scales of the two techniques. Although exchange coupling seems prevalent between the particles, we were not able to observe exchange bias in the composite systems. In studies of thin films it has also been found that exchange coupling can lead to an enhanced coercivity which is not related to the size of exchange bias.³⁹ In the present case, the absence of exchange bias is probably due to rather small anisotropies of the nanoparticles on an absolute scale. This

implies that the γ -Fe₂O₃ particles can drag the sublattice magnetization of the antiferromagnets around due to the coupling between the particles. This is seen as an effect to the coercivity of the ferrimagnetic particles, but the anisotropy of the antiferromagnetic particles is too small to result in shifted hysteresis loops.

VI. CONCLUSIONS

The present studies have shown that during drying both suspensions of nanoparticles of the same material and nanoparticles of different materials, a strong magnetic interparticle interaction can be established. Such interactions play an important role for the coercivity and the superparamagnetic relaxation of the nanoparticles. The results also show that the way in which the nanopowders are dried can have a decisive influence on the magnetic properties. The effects can be ex-

plained by exchange coupling of neighboring particles in close contact. We suggest that the different influence of the NiO and CoO nanoparticles on the relaxation of iron oxide nanoparticles is related to a difference in magnetic anisotropy of the NiO and CoO particles.

ACKNOWLEDGMENTS

We thank L. Lilleballe for sample preparations, H. K. Rasmussen for help with Mössbauer measurements, and F. Grumsen for TEM micrographs. The Danish Technical Research Council (“Nanomagnetism” framework programme) and the Danish Natural Sciences Research Council (framework programme 51-00-0363 and DANSCATT) have financially supported the work. The neutron diffraction measurements were performed at the Swiss Spallation Neutron Source, Paul Scherrer Institute, Villigen, Switzerland.

*Present address: School of Materials and Metallurgy, Northeastern University, Shenyang 110004, China.

- ¹W. Luo, S. R. Nagel, T. F. Rosenbaum, and R. E. Rosensweig, *Phys. Rev. Lett.* **67**, 2721 (1991).
- ²C. Djurberg, P. Svedlindh, P. Nordblad, M. F. Hansen, F. Bødker, and S. Mørup, *Phys. Rev. Lett.* **79**, 5154 (1997).
- ³H. Mamiya, I. Nakatani, and T. Furubayashi, *Phys. Rev. Lett.* **80**, 177 (1998).
- ⁴T. Jonsson, P. Svedlindh, and M. F. Hansen, *Phys. Rev. Lett.* **81**, 3976 (1998).
- ⁵Y. Sun, M. B. Salamon, K. Garnier, and R. S. Averback, *Phys. Rev. Lett.* **91**, 167206 (2003).
- ⁶C. J. W. Koch, M. B. Madsen, S. Mørup, G. Christiansen, and L. Gerward, *Clay Miner.* **34**, 17 (1986).
- ⁷M. F. Hansen, C. B. Koch, and S. Mørup, *Phys. Rev. B* **62**, 1124 (2000).
- ⁸S. Mørup, M. B. Madsen, J. Franck, J. Villadsen, and C. J. W. Koch, *J. Magn. Magn. Mater.* **40**, 163 (1983).
- ⁹C. W. Ostefeld and S. Mørup, *Hyperfine Interact.* **5**, 83 (2002).
- ¹⁰C. Frandsen and S. Mørup, *J. Magn. Magn. Mater.* **266**, 36 (2003).
- ¹¹F. Bødker, M. F. Hansen, C. B. Koch, and S. Mørup, *J. Magn. Magn. Mater.* **221**, 32 (2000).
- ¹²S. Mørup and E. Tronc, *Phys. Rev. Lett.* **72**, 3278 (1994).
- ¹³S. Mørup, *Europhys. Lett.* **28**, 3278 (1994).
- ¹⁴M. F. Hansen and S. Mørup, *J. Magn. Magn. Mater.* **184**, 262 (1998).
- ¹⁵F. Luis, F. Petroff, J. M. Torres, L. M. García, J. Bartolomé, J. Carrey, and A. Vaurès, *Phys. Rev. Lett.* **88**, 217205 (2002).
- ¹⁶M. F. Hansen and S. Mørup, *Phys. Rev. Lett.* **90**, 059705 (2003).
- ¹⁷S. Mørup, F. Bødker, P. V. Hendriksen, and S. Linderoth, *Phys. Rev. B* **52**, 287 (1995).
- ¹⁸D. Fiorani, J. L. Dormann, R. Cherkaoui, E. Tronc, F. Lucari, F. D’Orazio, L. Spinu, M. Nogue, A. Garcia, and A. M. Testa, *J. Magn. Magn. Mater.* **196-197**, 143 (1999).
- ¹⁹J. Nogués and I. K. Schuller, *J. Magn. Magn. Mater.* **192**, 203 (1999).
- ²⁰A. E. Berkowitz and K. Takano, *J. Magn. Magn. Mater.* **200**, 552 (1999).

- ²¹J. A. Borchers, R. W. Erwin, S. D. Berry, D. M. Lind, J. F. Ankner, E. Lochner, K. A. Shaw, and D. Hilton, *Phys. Rev. B* **51**, 8276 (1995).
- ²²P. J. van der Zaag, Y. Ijiri, J. A. Borchers, L. F. Feiner, R. M. Wolf, J. M. Gaines, R. W. Erwin, and M. A. Verheijen, *Phys. Rev. Lett.* **84**, 6102 (2000).
- ²³V. Skumryev, S. Stoyanov, Y. Zhang, G. Hadjipanayis, D. Givord, and J. Nogués, *Nature (London)* **423**, 850 (2003).
- ²⁴H. Zeng, J. Li, J. P. Liu, Z. L. Wang, and S. Sun, *Nature (London)* **420**, 395 (2002).
- ²⁵J. Sort, J. Nogués, X. Amils, S. Surinach, J. S. Munoz, and M. D. Baro, *Appl. Phys. Lett.* **75**, 3177 (1999).
- ²⁶J. Sort, J. Nogués, X. Amils, S. Surinach, J. S. Munoz, and M. D. Baro, *J. Magn. Magn. Mater.* **219**, 53 (2000).
- ²⁷T. A. Anhøj, C. S. Jacobsen, and S. Mørup, *J. Appl. Phys.* **95**, 3649 (2004).
- ²⁸L. Néel, *Ann. Geophys. (C.N.R.S.)* **5**, 99 (1949).
- ²⁹W. F. Brown, Jr., *Phys. Rev.* **130**, 1677 (1963).
- ³⁰S. Mørup, C. Frandsen, F. Bødker, S. N. Klausen, K. Lefmann, P.-A. Lindgård, and M. F. Hansen, *Hyperfine Interact.* **144/145**, 347 (2002).
- ³¹S. N. Klausen, P.-A. Lindgård, K. Lefmann, F. Bødker, and S. Mørup, *Phys. Status Solidi A* **189**, 1039 (2002).
- ³²F. Bødker and S. Mørup, *Europhys. Lett.* **52**, 217 (2000).
- ³³F. Bødker, M. F. Hansen, C. B. Koch, K. Lefmann, and S. Mørup, *Phys. Rev. B* **61**, 6826 (2000).
- ³⁴M. F. Hansen, F. Bødker, S. Mørup, K. Lefmann, K. N. Clausen, and P.-A. Lindgård, *Phys. Rev. Lett.* **79**, 4910 (1997).
- ³⁵T. Jonsson, J. Mattsson, P. Nordblad, and P. Svedlindh, *J. Magn. Magn. Mater.* **168**, 269 (1997).
- ³⁶B. Martínez, X. Obradors, Ll. Balcells, A. Rouanet, and C. Monty, *Phys. Rev. Lett.* **80**, 181 (1998).
- ³⁷N. J. Gökemeijer, T. Ambrose, and C. L. Chien, *Phys. Rev. Lett.* **79**, 4270 (1997).
- ³⁸M. S. Lund, W. A. A. Macedo, Kai Liu, J. Nogués, Ivan K. Schuller, and C. Leighton, *Phys. Rev. B* **66**, 054422 (2002).
- ³⁹N. J. Gökemeijer, J. W. Cai, and C. L. Chien, *Phys. Rev. B* **60**, 3033 (1999).